The Journal of Engineering

The 9th International Conference on Power Electronics, Machines and Drives (PEMD 2018)

IET Journals
The Institution of Engineering and Technology

Probabilistic adaptive model predictive power pinch analysis (PoPA) energy management approach to uncertainty

eISSN 2051-3305
Received on 22nd June 2018
Accepted on 31st July 2018
E-First on 4th April 2019
doi: 10.1049/joe.2018.8154
www.ietdl.org

Nyong-Bassey Bassey Etim[1] ✉, Damian Giaouris[1], Haris Patsios[1], Shady Gadoue[2], Athanasios I. Papadopoulos[3], Panos Seferlis[3,4], Spyros Voutetakis[3], Simira Papadopoulou[3,5]

[1]*Newcastle University, School of Electrical and Electronic Engineering, Newcastle Upon Tyne, UK*
[2]*Aston University, School of Engineering and Applied Science, Birmingham, UK*
[3]*Chemical Process and Energy Resources Institute, Centre for Research and Technology Hellas, Thermi-Thessaloniki, Greece*
[4]*Department of Mechanical Engineering, Aristotle University of Thessaloniki, Thessaloniki, Greece*
[5]*Department of Automation Engineering, Alexander Technological Educational Institute of Thessaloniki, Thessaloniki, Greece*
✉ *E-mail: b.e.nyong-bassey1@ncl.ac.uk*

Abstract: This paper proposes a probabilistic power pinch analysis (PoPA) approach based on Monte–Carlo simulation (MCS) for energy management of hybrid energy systems uncertainty. The systems power grand composite curve is formulated with the chance constraint method to consider load stochasticity. In a predictive control horizon, the power grand composite curve is shaped based on the pinch analysis approach. The robust energy management strategy effected in a control horizon is inferred from the likelihood of a bounded predicted power grand composite curve, violating the pinch. Furthermore, the response of the system using the energy management strategies (EMS) of the proposed method is evaluated against the day-ahead (DA) and adaptive power pinch strategy.

1 Introduction

The significant impact of greenhouse gas emission on the ecosystem has continued to encourage the deployment of renewable energy sources (RES) such as wind turbines and solar panels, for distributed generation (DG). Additionally, the standalone RES serves as a good alternative for rural electrification [1]. However, due to the high variability of RES, the hybrid energy storage has been incorporated in the DG network to enhance reliability. Consequently, energy produced by fossil fuels is reduced by the RES penetration [2]. The combination of DG and hybrid energy storage systems (HESS) transforms the traditional power network from 'fit and forget' to a more dynamical and multi-purpose system. Energy can also flow in multiple directions and in various forms (like electrical and thermal) [3]. Therefore, energy management strategies (EMS) with active control of the HESS are desirable but introduce significant challenges.

Power pinch analysis (PoPA) [4] is a graphical method which enables the systematic identification of energy recovery opportunities in hybrid RES. It considers power demand and supply requirements with respect to time in the form of the power grand composite curves (PGCC) to identify inflection points (called pinches) where power demands must be satisfied by external, non-RESs. The identification of pinch points allows the development of EMS which support efficient internal energy recovery so that the use of non-renewable energy can be avoided. The PGCC have mainly been used to identify energy needs in deterministic scenarios to enhance reliability and optimal operation of HESS. An EMS, using the PoPA graphical tool, was proposed in an isolated hybrid micro-grid to identify the minimum energy targets required for storage and consequently the needed outsourced electricity to cater for energy deficit in a hybrid system [4]. The operation cost and emission impact of diesel generator was reduced after integration with renewable energy from wind turbines and photovoltaic (PVs) panels using PoPA in [5]. In [2], PoPA was presented as an enhanced graphical tool, exploiting the demand and supply PGCC of an isolated hybrid micro-grid in a novel way and in addition, load shifting has been employed using PoPA in [6]. The PGCCs were used in the form of a cascaded demand-supply tables and as a graphical tool to identify peak demand, thereafter time shifted to off-peak period, in a bid to enhance grid reliability. More recently, [7] proposed a chance constrained optimisation in a pinch analysis framework for RES sizing to meet a predefined reliability to uncertainty, thereafter, Monte–Carlo simulation (MCS) was used to verify the approach.

In [8], the shaping of the PGCC was implemented online, for the first time, using the day-ahead (DA) rolling horizon model predictive approach to compute the open loop control sequence offline for the activation of the energy assets. The EMS which consequently shapes the system's PGCC in order to avoid violating the pinch point is pre-determined in the predictive horizon and implemented on the system online. However, the open loop approach becomes insufficient in handling forecast error due to uncertainty, which causes a mismatch between the estimated and real load and weather data profile.

The PoPA, therefore, benefits the operator as it serves as a minimalist conservative technique for planning in advance, demand, and power supply schedule using the PGCC. However, weather intermittency as well as the stochastic consumers load usage pattern, pose risk on both the reliability and infrastructure sustainability of the assets. Therefore, incorporating the chance constraint method in the EMS for energy recovery is essential since the deterministic models are often employed with the PoPA which consequently impact on reliability.

This paper presents two adaptations of the original method presented in [8]. First, the prediction horizon is adapted in a receding model predictive framework based on the prediction error. Second, a probabilistic method, MCS is proposed for investigating the robustness against load/weather uncertainty.

2 Methodological framework

2.1 Hybrid energy storage systems modelling

As a case study, the HESSs comprise renewable energy generation via solar panels (PV), fuel cell (FC), and electrolyser (EL), battery (BAT), water (WT), and hydrogen tank (HT), with a backup diesel generator (DSL). The HESS parameters are the same as [3] for consistency. The state of the accumulator *SOAcc* is expressed mathematically as follows; (see (1))

$$SOAcc_l^{n,m}(t) = SOAcc_l(t-1) + \frac{\sum_{x1 \in RS} ConvF_{l \leftarrow x1}^{j}(t) - \sum_{x2 \in RS} ConvF_{l \leftarrow x2}^{j}(t)}{c_l} \times \Delta t \quad (1)$$

The flow of electrical energy or material is defined as follows:

$$F_{l \rightleftarrows RS^{conv}}^{j} = \varepsilon_i(t) \times \delta Q_i^j(t), i \in \{x1, x2\} \quad (2)$$

where ε_i (t) is a binary variable of the dispatchable asset state, δ is used for varying the magnitude of energy or material [ineq] converted by the ith dispatchable unit [3]. Also, $x1$ and $x2$ are energy transforming resources $Rs^{conv} \in [FC, EL, LD, DSL, PV]$ which, respectively, supply and consume the energy in an energy storage system l. In addition, the existence of an edge (signified by '←' and '→' which establishes a path for in and out flow of energy, respectively), is represented by the logical binary variable ε_i $(t) \in [0, 1]$. Furthermore, ε_i (t) is inferred from the state of the storages $SOAcc(t)$, where C_l is storage capacity and subscript $l \in [BAT, HT, WT]$ refers to the energy storage system while m, n superscripts refer to the actual and estimated values of the HESS.

$$\varepsilon_i(t) = L(\varepsilon_i^{Avl}(t), \varepsilon_i^{\text{Req}}(t), \varepsilon_i^{Gen}(t)) \quad (3)$$

where superscripts Avl, Req, and Gen in ε_i represent availability, request, and override are sub-logical conditions, respectively, pertaining to l, which must be satisfied in order to activate the dispatchable assets [3].

2.2 Power pinch for hybrid energy storage management

The BAT acts as the primary storage and the excess energy in the system is utilised by the EL to produce hydrogen, while the BAT is charged (state-of-charge ($\boldsymbol{SOAcc_{BAT}}$) > **90%**). The FC in turn charges the battery using the stored hydrogen when $\boldsymbol{SOAcc_{BAT}}$ is below the minimum set limit (0%). The energy management system works to keep $\boldsymbol{SOAcc_{BAT}}$ of the battery within the acceptable region, the (**30%** < $\boldsymbol{SOAcc_{BAT}}$ < **90%**), to ensure reliability and optimum operation of the HESS.

The main principles of the PoPA concept, as applied in power generation systems, are illustrated in Fig. 1. An accumulator (e.g. hydrogen tank) stores excess energy from a converter (e.g. PV) due to saturation of another converter (e.g. battery's state of charge $SOAcc_{BAT}$ > Up). Similarly, another converter (e.g. Fuel cell) utilises the stored hydrogen to maintain the $SOAcc_{BAT}$ from falling below a lower limit ($SOAcc_{BAT}$ < Lo). When maintenance of the system within these limits becomes impossible, they are violated. This is all shown through a plot of $SOAcc_{BAT}$ with respect to time (continuous black line in Fig. 1) which is called the power grand composite curve (PGCC) of the system. In the case of the Lo limit, the PGCC indicates the amount of minimum outsourced electricity supply (MOES) required (e.g. through non-renewable resources) in order to move and keep the curve above it. In the case of the Up limit, the PGCC indicates the amount of minimum absorbed electricity (MAE) that needs to be dumped, which is also undesirable. By shifting the entire PGCC up or down (red dot-dashed line in Fig. 1), the point in time where the PGCC touches the Lo or Up lines is called the pinch point. The new, shifted curve indicates the energy storage targets at each instance in order to operate within the desired limits. The initiation or termination of the appropriate converters allows the generation of an overall EMS that best matches the shifted curve. However, realising the PoPA successfully via DA strategy requires accurate load and weather data which is often not the case due to uncertainty. The effect of the uncertainty $\Delta H_{1,2}$ causes a mismatch between the actual and predicted $SOAcc$ parameters as shown in Fig. 2. Therefore, violation of the upper and lower pinch may occur.

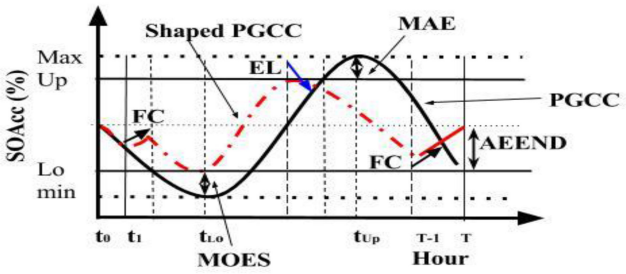

Fig. 1 *PGCC shaping utilising DA-PoPA without uncertainty [9]*

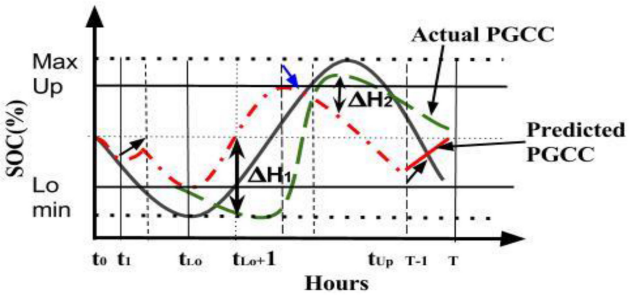

Fig. 2 *PGCC shaping utilising DA-PoPA with load and weather uncertainty [9]*

2.3 Monte–Carlo simulation for uncertainty

The MCS has mostly been utilised to obtain probabilistic insight in order to negate uncertainty via robust sizing [7], energy reserve planning [10], and peak load shaving [11], as well as economic risk analysis [12] in power systems. Furthermore, MCS is favourable for low capacity planning in low-voltage grid to which the simultaneity factor often employed in high-medium reserve planning becomes less accurate.

3 Adaptive power pinch with Monte–Carlo simulation for energy management

The chance constraint sizing approach presented in [7], for minimum solar panel array area utilised in the PoPA framework, primarily targeted reliability of the deterministic load demand being met as well as the battery being charged. Furthermore, energy management of BAT in the event that the battery becomes fully charged and the utilisation of the excess energy were not discussed. Thus, this paper presents an adaptation of the works of [4] and [7, 9] by defining the robust adaptive energy management algorithm in a probabilistic chance constrained framework. Furthermore, the excess energy in the system, represented by overcharging the BAT ($SOAcc_{BAT}^{n} > 90\%$) and energy recovered as well as over discharging the BAT ($SOAcc_{BAT}^{n} < 30\%$), is considered in the chance constraints evaluated with the MCS.

The MC sampling is performed iteratively in the prediction horizon to determine the likelihood of the PGCC, violating constraints (5)–(8). The pinch set points are expressed probabilistically using the chance constraint. Therefore, two PGCC form a (upper and lower) closed bounds within which the uncertainty is defined. Consequently, the EMS which infers the optimal control sequence in a prediction horizon at time step, $k \in [1: 24]$. The EMS effected in advance at the beginning of the receding control horizon keeps the system within the desired operating limits, while incorporating robustness to uncertainty, as follows;

$$SOAcc_l^{m(j)}(k+1)^{tr} := \min_{U_c} \sum_{K=1}^{T-1} \left[\sum_{j=1}^{n} f(\varepsilon_i(k),\ SOAcc_l^{m(j)}(k), U_c(k)) \right] \quad (4)$$

$$\varepsilon_{FC}^{Gen}(k) + \varepsilon_{EL}^{Gen}(k) \leq 1 \quad (5)$$

$$SOAcc_l^n(k_1) \cong SOAcc_l^m(T) \quad (6)$$

$$S_{Lo}^l \leq SOAcc_l^m(k) \leq S_{Up}^l \quad (7)$$

$$F_{\min} \leq F_{BAT \leftrightarrow Conv} \leq F_{\max}, Conv \in [FC, EL] \quad (8)$$

where S_{LO}^l and S_{Up}^l are the lower and upper operational limits of the Battery's state of charge and k_1 and T are the first hour (01:00 h) and last (24:00 h) of a 24 h (daily horizon) interval, respectively. $U_c(k)$ is the determined EMS resulting from PoPA minimum energy targeting which controls the flow of power and activation of the FC and EL. Therefore, $SOAcc_l^{m(j)}(k+)^{tr}$ is a transposed vector, which comprises the posterior distribution of the state of charge of the battery for each consumer load, sampled randomly from the priori distribution.

The constraints in (5) prevent both FC and EL from activating at the same instance. Equation (6) maintains the available energy for the next day by activating EL or FC to match the energy required during the start of the day. Additionally, (7) and (8) are the pinch and device power rating constraints.

The PGCC targeting is exploited iteratively so as to achieve robustness and compensate for inconsistencies between the real and the estimated weather/load profile. The receding horizon model predictive control (RHMPC) PoPA, hence, employs a state feedback loop to adapt the model to the HESS. Thus, a closed loop is utilised and the estimated and real states are compared for discrepancy so as to achieve robustness to compensate for the weather/load uncertainty [9]. Hence, minimising the effect of uncertainty $\Delta H_{1,2}$ between the real and the estimated state of charge and the state feedback error due to uncertainty is re-computed as follows;

$$\Delta H(k|k) = |y^m(k) - y^n(k|k-1)| \quad (9)$$

where $y(k)$ is the output state measured at time k, and superscripts m, $n$refer to the real and the estimated state of charge, respectively.

Moreover, if $\Delta H_{1,2}$ is greater than the error threshold ξ at any sampling instance, the PoPA is repeated in the predictive horizon in order to determine the optimal control sequence from that instant until time T. The threshold error ξ is set at 5% to reduce the computational cost. The state of charge of the battery in the model for PGCC re-computation is updated as follows:

$$\text{If } \exists\, \Delta H(k) > \xi, \forall_k, Y^m(k) := f(Y^n(k|k-1)) \quad (10)$$

$$SOAcc_{BAT}^m(k|k) = SOAcc_{BAT}^m(k|k-1) \pm \Delta H(k) \quad (11)$$

The MCS is performed on the distribution $f(\varepsilon_i(k), SOAcc_l^{m(j)}(k), U_c(k))$ over $j\in$ [1: n] number of random demand load samples, each time the PGCC is recomputed in the prediction horizon. Furthermore, the probabilistic minimum energy target required to satisfy the load demand with a given reliability index for robustness is presented as follows;

The cumulative distribution function of the random variable $SOAcc_{BAT}^m$ violating the lower limit is constrained by a chance factor α_1:

$$F(SOAcc_{BAT}^m) = Pr[SOAcc_{BAT}^m(k) \geq S_{\min}] \geq \alpha_1, \alpha_1 \in [0,1] \quad (12)$$

Therefore, the probability of violating the lower operating limit for BAT is constrained as follows:

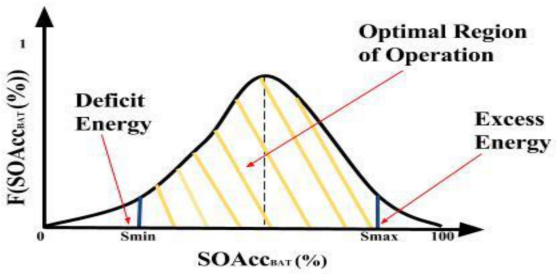

Fig. 3 *Probability distribution function of the dependent random variable* $SOAcc_{BAT}^m(\%)$

$$Pr[SOAcc_{BAT}^m(k) \leq S_{\min}] \geq 1 - \alpha_1 \quad (13)$$

Similarly, the chance of violating the upper pinch limit is as follows:

$$Pr[SOAcc_{BAT}^m(k) \geq S_{\max}] \leq \alpha_2, \alpha_2 \in [0,1] \quad (14)$$

$$Pr[SOAcc_{BAT}^m(k) \leq S_{\max}] \geq 1 - \alpha_2 \quad (15)$$

Therefore, the desired operating range for $SoA_{BAT}^m(k)$ with respect to the chance constraint is expressed with the inverse cumulative distribution function (CDF) in (13):

$$F_{SOAcc_{BAT}^m}^{-1}(\alpha_1) \leq f(SOAcc_{BAT}^m) \leq F_{SOAcc_{BAT}^m}^{-1}(1-\alpha_2) \quad (16)$$

Similarly, the probability density function equivalent of the CDF for the desired operating region is shown in Fig. 3 and presented in (16) and (17). The shaded portion of Fig. 3 represents the desired operating region while the lower and upper tails.

$$\int_{S\min}^{S\max} f[SoAcc]d(SoAcc) = F(S\ \max) - F(S\ \min) \quad (17)$$

The decision variable U_c for the activation of the fuel cell and electrolyser based on the pinch analysis as a consequence of violating (2) and (3), respectively, is as follows;

$$U_c(k)\begin{Bmatrix} F_{BAT \leftarrow FC} & F_{SOAcc_{BAT}^m}^{-1}(\alpha_1) < S_{\min} \\ F_{BAT \rightarrow EL} & F_{SOAcc_{BAT}^m}^{-1}(1-\alpha_2) > S_{\max} \\ 0 & \text{Otherwise} \end{Bmatrix} \forall_{k \in [1:T-2]} \quad (18)$$

where $F_{SOAcc_{BAT}^m}^{-1}(\alpha_{1,2})$ is the inverse cumulative distribution of the randomly distributed variable $SoAcc_{BAT}^m(k)$.

Additionally, the MOES and MAE necessary for maintaining the lower and upper pinch points, respectively, are obtained as follows in (19) and (20), respectively:

$$MOSE: F_{BAT \leftarrow FC} = \left[S_{min} - F_{SOAcc_{BAT}^m}^{-1}(\alpha_1)\right] \times C_{BAT} \quad (19)$$

$$MAE: F_{BAT \rightarrow EL} = \left[F_{SOAcc_{BAT}^m}^{-1}(1-\alpha_2) - S_{max}\right] \times C_{BAT} \quad (20)$$

The EMS decision-making variable U_c in conjunction with the magnitude of energy flow determined in (16) and (17) satisfy the lower and upper pinch points with regard to the chance constraint (9)–(11) in an adaptive receding horizon model predictive framework. Similarly, the available electricity for the next day (AEEND) for life-cycle preservation is determined using the upper bound as follows:

$$\Pr\left[SOAcc_{BAT}^m(T) \cong SOAcc_{BAT}^n(k_1)\right] \geq (1-\alpha_2)\ \forall_T \quad (21)$$

Thus, AEEND: (see (22)) . Furthermore, the power management control sequence obtained with the MCS of the model is, therefore,

$$U_c(k) = \begin{Bmatrix} F_{BAT \leftarrow FC} & F^{-I}_{SOAcc^m_{BAT}}(1-\alpha_2) < SOAcc^n_{BAT}(k_1) \\ F_{BAT \leftarrow EL} & F^{-I}_{SOAcc^m_{BAT}}(1-\alpha_2) > SOAcc^n_{BAT}(k_1) \\ 0 & \text{Otherwise} \end{Bmatrix} \forall_{k \in [T-I]} \quad (22)$$

effected in the control horizon taking the overall risk of violating the utility pinch constraints into consideration.

4 Load demand and weather data

The historical household load demand profile with peak load of 1.5 KW and solar irradiance data corresponding to 54.9783°N, 1.6178°W are obtained from [13] and [14], respectively. The load profile data set consists of the aggregated power demand of uncontrollable appliances at each hourly time interval representing consumer's usage pattern. The historical load profile data set, A (j, k) collected over 365 days, at each hourly time step k, such that j = 1, 2, 3…365 is partitioned into disjointed groups of $A(j, k) = \{A_1, A_2, A_3, A_4\}$ [15]. Each group of load demand data set corresponds to the consumer's power usage pattern correlating to the four seasons [10]. Therefore, from the consumer's historical energy consumption profile as shown in Fig. 4, a probability distribution is deduced. In employing the MCS, the load demands are usually assumed to be normally distributed. However, in this work, a non-parametric kernel density estimator is used to estimate the underlying load demand distribution in each cluster (for each j at time step k). Furthermore, in order to validate the proposed approach, the actual load is randomly selected with uniform probability from the load demand distribution corresponding to the time instance (k). The DA PoPA and adaptive strategies utilising the average load for each season are compared against the proposed probabilistic PoPA method.

5 Uncertainty analysis of the HESS

The proposed method utilising the chance constrained power pinch for energy management is simulated in MATLAB based on 1000 samples randomly generated from a uniform distribution $A(j, k)$.

The chance constraint factors were both set to 1% during the simulation. Therefore, state of charge of the battery has a 98% probability of operating within the optimal region ($30\% \leq SOAcc^n_{BAT} \leq 90\%$). As shown in Fig. 5, the system PGCC is bounded, by both the probabilistic lower and upper PGCC. The response of the system over a period of 72 h is shown in Fig. 5. The red and blue lines in Fig. 5 are the lower and upper predicted PGCC based on the chance constraint. The yellow-dashed line represents the actual response of the system. The PGCC upper pinch violation at 40th hour accurately predicts the pinch during the first 72 h hence the EL is activated.

We compare three algorithms. The DA algorithm where uncertainty is not considered, the RHMPC-PoPA algorithm where the prediction error is corrected [9] and the MC-PoPA algorithm where uncertainty is considered.

From Table 1, the proposed method has a total of 319 upper pinch violations compared to the DA and RHMPC-PoPA with 603, 653. However, it has the most significant number of violations, 1374 and 1208, respectively, in both lower pinch zones ($SOAcc <$ 30% and $20\% < SOAcc < 30\%$).

Consequently, the RHMPC-PoPA has 1176 with the DA-PoPA having the least violations of 1094. The activation of the DSL accordingly correlates with the lower pinch violation, thus the proposed method activated the DSL more frequently, 576 times. Thi, however, is not significant compared to the 561 times the DSL was activated utilising the RHMPC-PoPA.

Furthermore, despite the DA-PoPA having the lowest DSL activation of 325 times, it does not truly reflect positive gains as these largely result from over-charging (upper pinch violation) and the stochastic dynamics of the actual load demand profile. Furthermore, the DA-PoPA exhibits lower participation in the energy recovery. The FC and EL are activated 79 and 205 times compared the MC-PoPA (194 and 882 times) and RHMPC (213 and 724 times). Evidently, the low frequency of activation is due to the DA targeting as the strategy does not account for energy mismatch caused by uncertainty within the horizon.

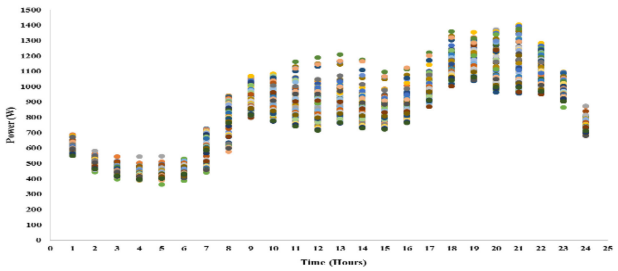

Fig. 4 *Load demand profile showing energy consumption pattern variability during winter*

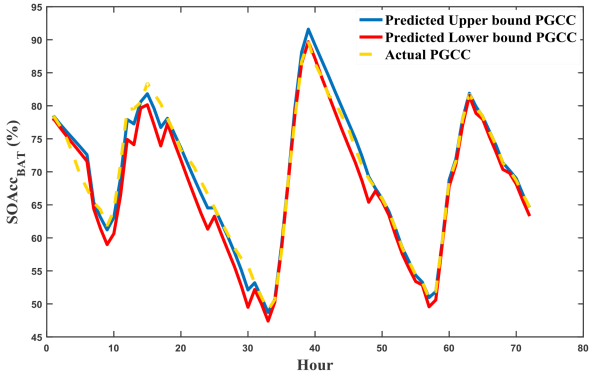

Fig. 5 *Response of the Battery's state of charge to MC-PoPA*

Table 1 Operational indices for 8760 h

Operational parameter	EMS		
	DA-PoPA	*RHMPC-PoPA*	*MC-PoPA*
FC attempt (cycles/year)	250	1687	2147
FC start-stop (cycles/year)	79	194	213
EL attempts (cycles/year)	205	882	724
EL start-stop (cycles/year)	205	882	717
PV start-stop (cycles/year)	7996	8031	8343
DSL start-stop (cycles/year)	325	561	576
Lower Pinch violation (counts/year)	1094	1176	1374
Lower Pinch violation (counts/year)20% < $SOAcc_{BAT}$ < 30%	998	1025	1208
Upper Pinch violation(counts/year)	764	729	417
Upper Pinch violation (counts/year)90% < $SOAcc_{BAT}$ < 100%	653	603	319

6 Conclusion

An adaptive power pinch analysis based on MCS for energy management of HESS, with respect to uncertainty, has been proposed. The stochastic analysis evidently showed the proposed method performed better in clipping the PGCC from violating the upper pinch. The proposed method was compared to the DA and adaptive PoPA, which utilised the average load. However, the DA PoPA which had the most upper violation consequently had a lowest lower pinch violation and DSL utilisation. The adaptive PoPA had a marginally better lower pinch violation compared to the proposed approach. Regardless of the better lower pinch

violation, the DA-PoPA is arguably sufficient only if the variance in energy target for the day is negligible and does not account for uncertainty. Hence, future work would investigate sensitivity of the methods with respect to several classes of load demand profiles.

7 Acknowledgments

The first author would like to acknowledgement Petroleum Development Technology Funds (PTDF), Nigeria for sponsoring his research in Energy management at Newcastle University, United Kingdom.

8 References

[1] Dorji, T., Urmee, T., Jennings, P.: 'Options for off-grid electrification in the Kingdom of Bhutan', *Renew. Energy*, 2012, **45**, pp. 51–58

[2] Ho, W.S., Khor, C.S., Hashim, H., *et al.*: 'SAHPPA: a novel power pinch analysis approach for the design of off-grid hybrid energy systems', *Clean Technol. Environ. Policy*, 2014, **16**, (5), pp. 957–970

[3] Giaouris, D., Papadopoulos, A.I., Ziogou, C., *et al.*: 'Performance investigation of a hybrid renewable power generation and storage system using systemic power management models', *Energy*, 2013, **61**, pp. 621–635

[4] Giaouris, D., Papadopoulos, A.I., Voutetakis, S., *et al.*: 'A power grand composite curves approach for analysis and adaptive operation of renewable energy smart grids', *Clean Technol. Environ. Policy*, 2015, **17**, (5), pp. 1171–1193

[5] Rozali, N.E.M., Alwi, S.R.W., Ho, W.S., *et al.*: 'Integration of diesel plant into a hybrid power system using power pinch analysis', *Appl. Therm. Eng.*, 2016, **105**, pp. 792–798

[6] Rozali, N.E.M., Alwi, S.R.W., Manan, Z.A., *et al.*: 'Cost-effective load shifting for hybrid power systems using power pinch analysis', *Energy Procedia*, 2014, **61**, pp. 2464–2468

[7] Norbu, S., Bandyopadhyay, S.: 'Power pinch analysis for optimal sizing of renewable-based isolated system with uncertainties', *Energy*, 2017, **135**, pp. 466–475

[8] Giaouris, D., Papadopoulos, A.I., Seferlis, P., *et al.*: 'Power grand composite curves shaping for adaptive energy management of hybrid microgrids', *Renew. Energy*, 2016, **95**, pp. 433–448

[9] Nyong-Bassey, B.E., Giaouris, D., Papadopoulos, A.I., *et al.*: 'Adaptive power pinch analysis for energy management of hybrid energy storage systems'. 2018 IEEE Int. Symp. on Circuits and Systems (ISCAS), May 2018, pp. 1–5

[10] Mavrotas, G., Florios, K., Vlachou, D.: 'Energy planning of a hospital using mathematical programming and monte carlo simulation for dealing with uncertainty in the economic parameters', *Energy Convers. Manage.*, 2010, **51**, (4), pp. 722–731

[11] Du, W.: 'Model validation by statistical methods on a monte-carlo simulation of residential Low voltage grid': '*Future communication, computing, control and management*' (Springer, Berlin, Heidelberg, Germany, 2012), pp. 93–98

[12] Da Silva Pereira, E.J., Pinho, J.T., Galhardo, M.A.B., *et al.*: 'Methodology of risk analysis by monte carlo method applied to power generation with renewable energy', *Renew. Energy*, 2014, **69**, pp. 347–355

[13] Available at http://data.ukedc.rl.ac.uk/simplebrowse/edc/efficiency/residential/LoadProfile/data, accessed 1 Nov. 2017

[14] Available at http://pvwatts.nrel.gov/pvwatts.php, accessed 1st Nov 2017

[15] Khan, Z.A., Jayaweera, D.: 'Approach for smart meter load profiling in monte carlo simulation applications', *IET Gener. Transm. Distrib.*, 2017, **11**, (7), pp. 1856–1864